INTEGRATION OF A MICROSTRIP PATCH ANTENNA WITH A TWO-DIMENSIONAL PHOTONIC CRYSTAL SUBSTRATE

K. Agi, K. J. Malloy, E. Schamiloglu, M. Mojahedi
Center for High Technology Materials
Electrical and Computer Engineering Department
University of New Mexico
1313 Goddard SE
Albuquerque, NM 87106, USA

E. Niver
Department of Electrical and Computer Engineering
New Jersey Institute of Technology
University Heights
Newark, NJ 07102, USA

ABSTRACT

We have experimentally and computationally studied the integration of a microstrip patch antenna with a two-dimensional photonic crystal substrate. This antenna was fabricated on a defect in the two-dimensional photonic crystal lattice that localized the energy under the patch antenna. The finite-difference time-domain method was employed to study the characteristics of this antenna. Measurements are in excellent agreement with calculations. The effects of finite size ground planes were also studied. This work can lead to a new design tool for integrating patch antennas with photonic crystal substrates.

Electromagnetics, 19:277 – 290, 1999

0272-6343 / 99 $12.00 + .00

1. INTRODUCTION

Photonic crystals are a class of periodic metallic, dielectric, or composite structures that exhibit transmission (pass) and reflection (stop) bands in their frequency response (Brown and McMahon, 1995; Joannopoulos et al., 1995). These bands in photonic crystals occur due to the constructive and destructive interference of the electromagnetic waves. For example, the stop band in a three-dimensional infinite crystal is referred to as a "forbidden" gap since the waves in *all* directions destructively interfere and are thus evanescent. The photonic crystals used in this work are fabricated by drilling holes in a dielectric host using standard machining techniques. If the periodicity in a photonic crystal is perturbed (by either removing or adding a material with a different dielectric constant), creating a "defect," a state is created in the forbidden gap where an electromagnetic mode is allowed and localization of the energy occurs (Joannopoulos et al., 1995).

Photonic crystals are currently being introduced in many novel microwave applications. For example, they are used as filters in microstrip lines (Radisic et al., 1998), as high-power microwave components (Agi et al., 1996), and as substrates for printed antenna structures (Brown et al., 1994; Kessler et al., 1996; Sigalas, et al., 1997; Yang et al., 1997). Theoretical descriptions of photonic crystals thus far have been limited to determining the dispersion curve in an infinitely periodic structure (Everitt et al., 1993). However, many of the applications listed above require the determination of the characteristics of a photonic crystal of finite size or with a finite ground plane. One effective approach to studying finite-sized crystals, as well as antenna applications of photonic crystals has been the finite-difference time-domain (FDTD) technique (Kunz and Leubbers, 1993; Taflove, 1995). This technique is implemented in this work.

Microstrip patch antennas are, on the other hand, well understood and have found applications in communication systems as well as many other systems that require compact antenna structures (Pozar and Schaubert, 1995). The conventional microstrip antenna is a metallic patch of arbitrary shape that is placed a certain distance, typically less than 0.01λ, above a metallic ground plane. They are typically excited using a coaxial probe from the ground plane as shown in the inset of Figure 1, or by a microstrip line in the plane of the antenna (Pozar and Schaubert, 1995). Due to their resonant nature, however, microstrip patch antennas are inherently narrowband. Although many techniques have been presented to effectively increase the bandwidth of the patch antenna, many of the

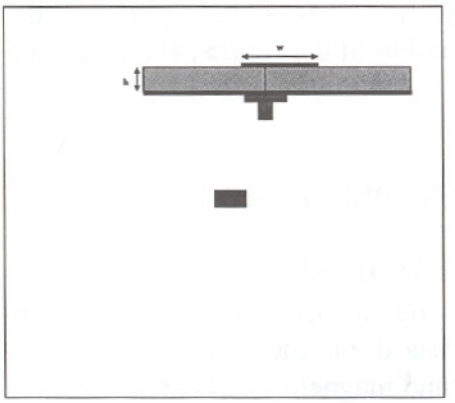

Figure 1(a)

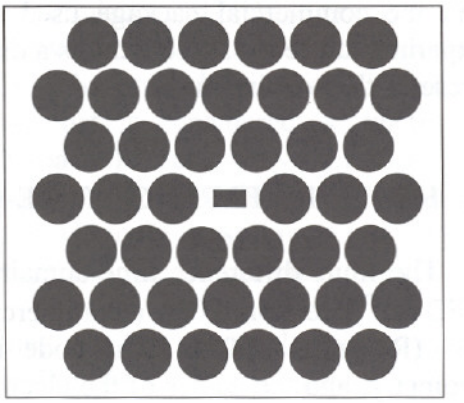

Figure 1(b)

Figure 1(a). Conventional patch antenna with a coaxial probe excitation (inset). (b). Two-dimensional photonic crystal that is integrated with the conventional patch.

solutions are complicated or require multi-layer structures (Pozar and Schaubert, 1995).

One of the simplest methods for increasing the bandwidth of a patch antenna is to increase the thickness of the dielectric substrate (Pozar and Schaubert, 1995). The increase in the dielectric thickness, however, results in the excitation of substrate and surface modes that remove energy from the main radiation lobe. If a photonic crystal is designed such that the frequency of the substrate mode overlaps the stop band frequencies, the excited substrate mode exponentially decays, reducing the energy lost into the substrate. In a crystal of infinite extent, the substrate mode would be evanescent and no energy would be lost. Yang et al., (Yang et al., 1997) originally proposed that high-gain antenna structures could be obtained by printing an antenna on a *two-dimensional* photonic crystal. In this work, two-dimensional photonic crystals are employed as a means of eliminating the substrate and surface modes in the patch antenna. In addition, the two-dimensional photonic crystal antenna structure is fabricated with a defect in the periodicity at the patch antenna location, confining the energy under the antenna. It is anticipated that this energy confinement would lead to a more efficient antenna structure.

The remainder of the paper is organized as follows. Section 2 will provide a brief description of the finite-difference time-domain method

and the commercial package used. Section 3 is a description of the experimental set-up. Section 4 is a discussion of the results, and Section 5 presents the conclusions.

2. FINITE-DIFFERENCE TIME-DOMAIN METHOD

The finite-difference time-domain (FDTD) code used in this work is XFDTD® (Version 4.06), a commercial code available through Remcom, Inc. (Remcom, 1997). The code is based on the standard Yee cell geometry, and the values of the electric and magnetic fields are calculated in consecutive time steps (Kunz and Leubbers, 1993). The utility of the program is manifested in the ability to calculate S-parameters (Kunz and Leubbers, 1993). The Cartesian coordinate system is employed and the two antennas compared in this work are shown in Figure 1 with the coaxial probe excitation shown in the inset. Two sets of simulations are performed. The initial sets of simulations are used to validate the code through experimental verification. The second sets of simulations are used to compare a conventional patch antenna with one that is integrated with a two-dimensional photonic crystal. Specifically, the effects of a finite ground plane will be investigated.

For the initial sets of simulations, the patch has a width of 8 mm in the x-direction and a length of 4.14 mm in the y-direction. The antenna geometry is broken up into a grid of Δx=0.4 mm, Δy=0.414 mm and Δz=0.25 mm in a space of 75x50x25 cells. The width of the antenna is 20Δx cells and the length of the antenna is 10Δy cells. The substrate in the FDTD calculation is 1.25 mm therefore occupying 5 cells in the z-direction with a dielectric constant of 10.2. The antenna is excited 1.66 mm centered from the bottom edge of the antenna. The time step is taken to be 0.6294 psec, which is set to the Courant limit for a general three-dimensional grid (Remcom, 1998). The ground plane is assumed to be infinite in extent. All other boundaries are set to be absorbing (Liao type).

For the second sets of simulations, the size of the FDTD space is increased such that the effects of the two-dimensional photonic crystal can be studied. The patch has a width of 8 mm in the x-direction and a length of 4 mm in the y-direction. The antenna geometry is broken up into a grid of Δx=0.1 mm, Δy=0.1 mm and Δz=0.4233 mm in a space of 120x135x35 cells. The substrate in the FDTD calculations is 1.27 mm thick, thereby occupying 3 cells in the z-direction and has a dielectric constant of 10.2. The time step is taken to be 1.211 psec, which is again set to the Courant limit for a general three-dimensional grid. For the modeling of the ground

plane, two cases are considered in this simulation. The first case is where the substrate is placed directly on the lower boundary, where the boundary is a perfect electric conductor (PEC). The ground plane in this case is infinite in extent. The second case that is considered is where the substrate is suspended in the FDTD space 10 cells above an absorbing boundary and a finite PEC layer is used as a ground plane. In both cases all remaining boundary conditions are set to be absorbing (Liao type). With the simulations mentioned above, the finite ground plane effects can be investigated.

The excitation source of the antenna is a Gaussian pulse with a width of 121 psec. The coaxial probe excitation of the antenna is shown on the inset of Figure 1. It was found that a thin wire was the best type of excitation suited for obtaining reasonable agreement with the experimental results. For the initial set of simulations, the code was run for 10,000 time steps that took approximately thirty minutes on a Pentium Pro, 300 MHz machine with 256 MB of RAM. For the second set of simulations, the code ran for approximately 5 hours on the same machine.

3. EXPERIMENTAL SET-UP

Two antennas were built for measurement. Both had a width in the x-direction of 8 mm and a length in the y-direction of 4.14 mm and were fabricated on a RT-Duroid 6010 substrate with a dielectric constant of 10.2. The thickness of both substrates was 1.27 mm (50 mils). The first antenna had a uniform dielectric substrate as shown in Figure 1(a), and the second antenna had the two-dimensional photonic crystal integrated, which was obtained by drilling holes into the substrate as shown in Figure 1(b). The photonic crystal substrate is a triangular lattice with lattice constant of 1.38 cm and a hole diameter of 1.27 cm and was designed to have a gap at approximately 9 GHz (Joannopoulos et al., 1995). This gap design is based on a photonic crystal that is infinite in extent in the transverse direction. The exact mode pattern of the grounded microstrip structure in a two-dimensional periodicity is currently under investigation.

The antenna pattern measurements were performed at the New Jersey Institute of Technology's anechoic chamber. An HP8340A sweep generator was used to excite the antenna structures and a Boonton 4200 power meter in conjunction with an X-band horn antenna was used to detect the radiation. The standard gain horn antenna was placed approximately 4.5 m away from the transmitter. The transmitting antenna was attached to a computer controlled rotary stage such that pattern

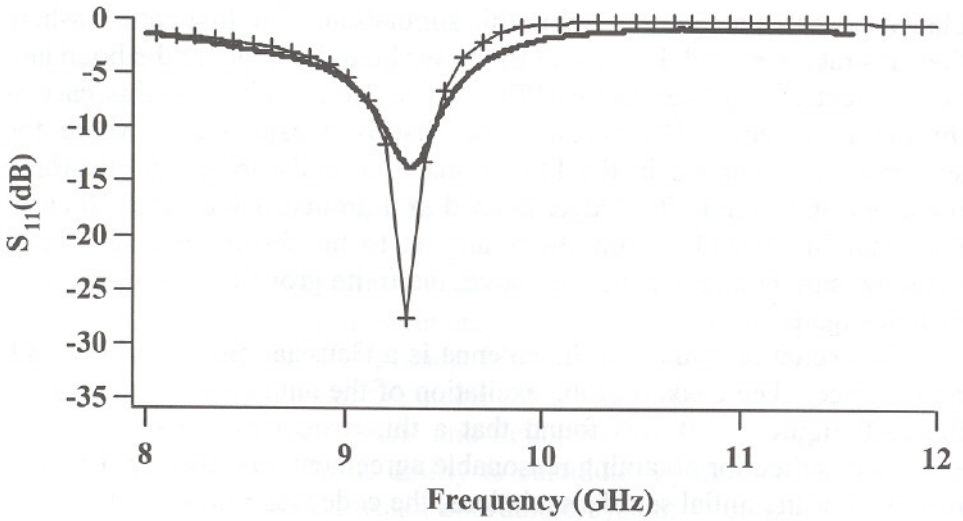

Figure 2. S_{11} measured (solid line) using a network analyzer and calculate (line with markers) using FDTD. There is excellent agreement between the calculations and the experiments.

measurements could be made. The excitation frequency for the antennas was determined by measuring the minimum return loss (S_{11}) using an HP8510 network analyzer.

4. RESULTS

The network analyzer measurements are compared to the FDTD calculation for the conventional patch antenna in Figure 2. In Figure 2, the solid line is S_{11} measured using the network analyzer and the line with the markers are the calculated results using XFDTD®. The calculated results are based on the first set of simulations and are in excellent agreement with the experiment. The first step is establishing the effects of a finite ground plane on the characteristics of a conventional (no photonic crystal substrate) patch antenna. Figure 3 is the result of the second simulation where a finite ground plane is compared to the infinite ground plane for a conventional patch antenna. Recall that the second simulation has a coarser grid as compared to the first simulation, such that the effects of a large ground plane and the photonic crystal could be investigated. The solid line is the infinite ground plane and the dashed line is the finite ground plane. Note that there is a slight increase in the resonance

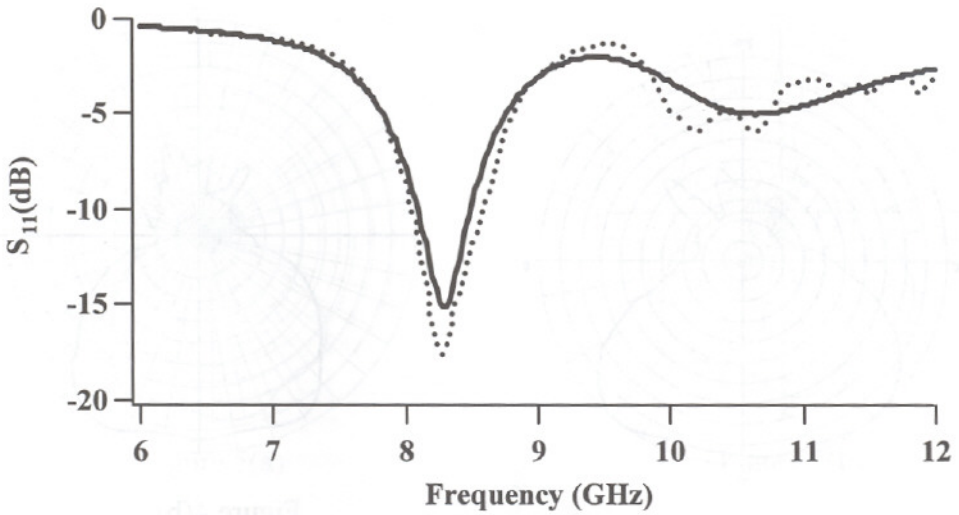

Figure 3. S_{11} calculated using FDTD for a conventional (no PC substrate) patch antenna investigating the effects of a finite ground plane. The solid line is an infinite ground plane and the dashed line is a finite ground plane. Note that the bandwidth of the resonance is slightly increased, the depth is slightly increased for a finite sized ground plane.

bandwidth of the finite crystal and a 4.5 dB increase in the depth of the resonance. However, there is no variation in the resonant frequency. In addition, the finite ground plane causes off-resonance ringing.

The second step is to compare the effect of the size of the ground plane on a conventional patch antenna without a photonic crystal substrate and a patch antenna with a photonic crystal substrate as shown in Figure 1. Figure 4 shows the measured pattern of the conventional patch antenna as a function of the size of the ground plane. Note that as the size of the ground plane is increased, the effect is a variation in the back lobe level. The lobes in a microstrip antenna pattern are due to the finite size of the ground plane. Given an infinite ground plane, there would be no back lobes. Figure 4(a) is the 5" square ground plane. Note that the scale on each antenna pattern measurement is 2 dB/division. For the 5" square ground plane in Figure 4(a), the maximum back lobe is 9 dB below the main beam and occurs at approximately 310°. For the 6" square ground plane in Figure 4(b), the maximum back lobe is 11 dB below the main beam and is at 290°. For the 9" square ground plane in Figure 4(c), the maximum back lobe is 10 dB below the main beam at 240°. Figure 5

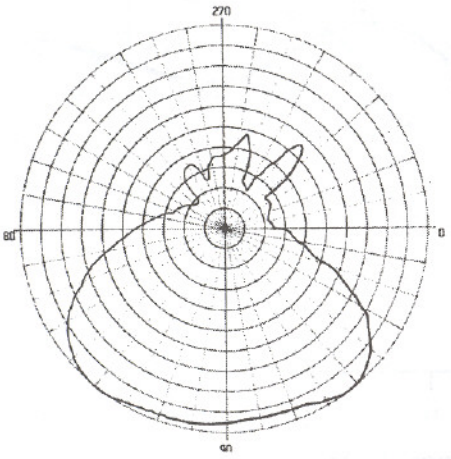

Figure 4(a)

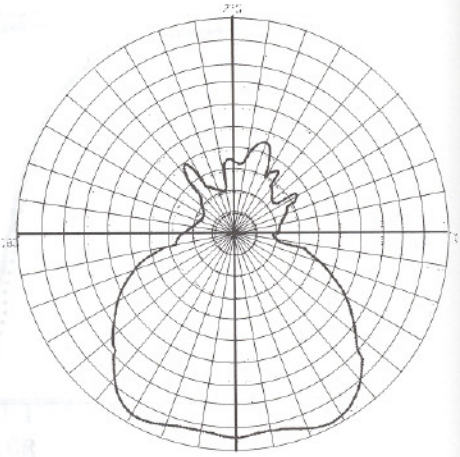

Figure 4(b)

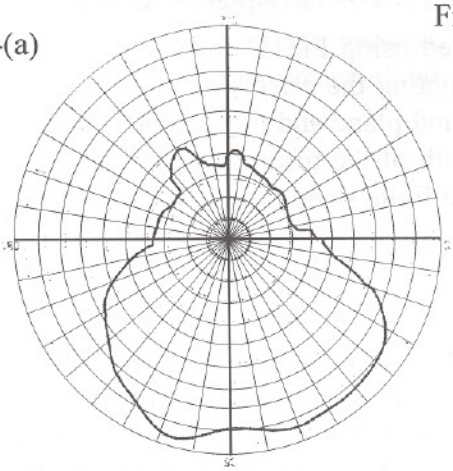

Figure 4(c)

Figure 4. Measured antenna pattern for various sized ground planes for a conventional patch antenna. (a). 5" ground plane, (b). 6" ground plane, (c). 9" ground plane.

presents the measured antenna patterns for the patch antenna with the two-dimensional photonic crystal incorporated as shown in Figure 1(b). For the 5" square ground plane in Figure 5(a), the maximum back lobe is 13 dB below the main beam at approximately 285°. For the 6" square ground plane in Figure 5(b), the maximum back lobe is 11 dB below the main beam at 265°. For the 9" square ground plane in Figure 5(c), the

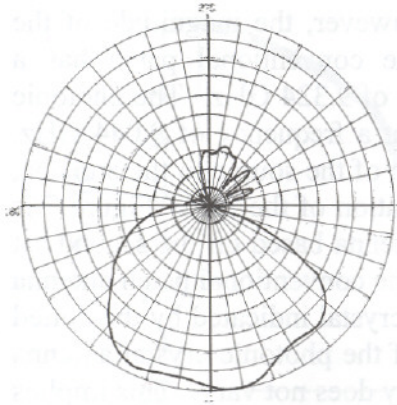

Figure 5(a)

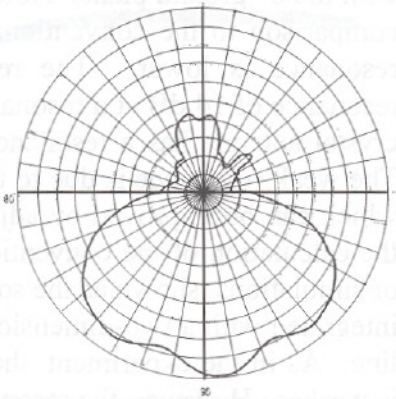

Figure 5(b)

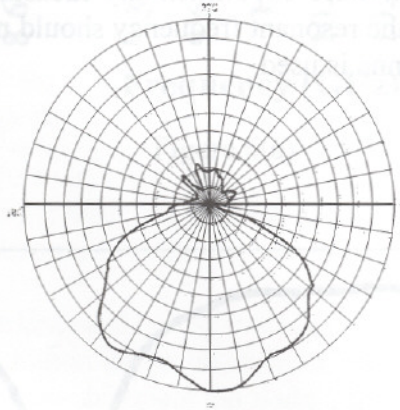

Figure 5(c)

Figure 5. Measured antenna pattern for two-dimensional photonic crystal integrated with a conventional patch antenna with varying sized ground plane. (a). 5" ground plane, (b). 6" ground plane, and (c). 9" ground plane. Note that the back lobes are significantly reduced as compared to the conventional patch antenna pattern shown in Figure 4.

maximum back lobe is 15 dB below the main beam at 250°. Therefore, the addition of the two-dimensional photonic crystal to the conventional patch antenna reduces the back lobe levels for the ground plane sizes considered here. Figure 6(a) is the S_{11} measurement for the conventional patch antenna. The resonant frequency of the conventional antenna is not a function of the size of the ground plane. On the other hand, Figure 6(b) is the S_{11} measurement for the two-dimensional photonic crystal antenna

with the 6" ground plane. Note that the antenna resonance is broadened in comparison to the conventional antenna, however, the magnitude of the resonance is lower. The response of the conventional patch has a resonance of 14 dB at a resonance frequency of 9.324 GHz. The photonic crystal antenna has a resonance of 7.5 dB at a frequency of 9.044 GHz. The weak resonance is due to the poor match of the source to the antenna, which can be improved by adjusting the location of the feed. Figure 7 is the calculation of the conventional patch antenna based on the second set of simulations, shown as the solid line, and the conventional patch antenna integrated with a two-dimensional photonic crystal indicated by the dotted line. As in the experiment, the resonance of the photonic crystal antenna is weaker. However, the resonance frequency does not vary. This implies that the antennas that were experimentally measured were not identical. Therefore, a shift in the resonant frequency should not be expected when a photonic crystal antenna is used.

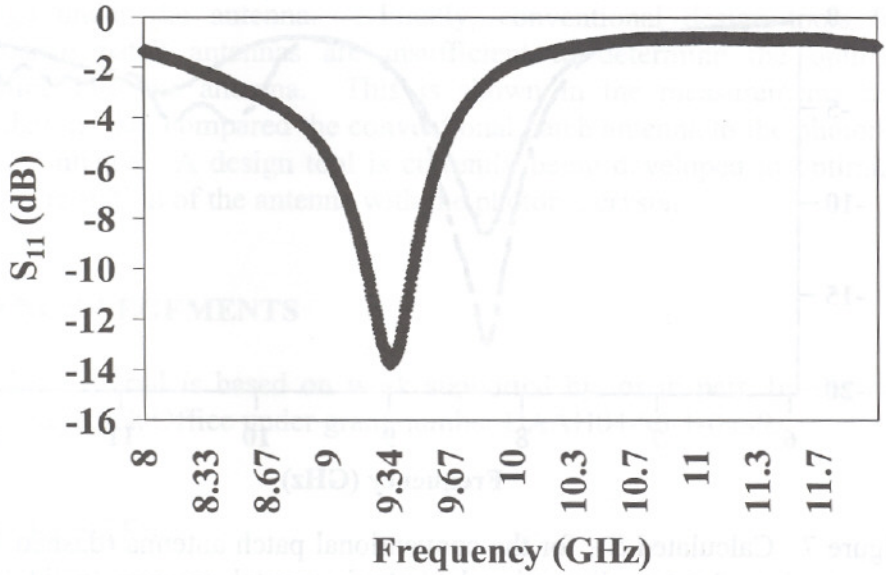

Figure 6(a)

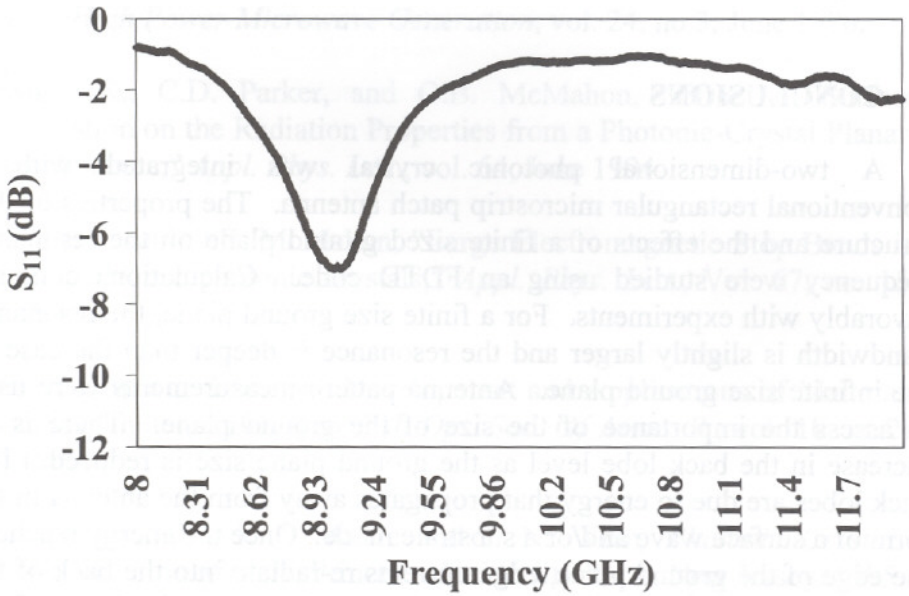

Figure 6(b)

Figure 6(a). Measured S_{11} for conventional microstrip patch antenna. (b). Measured S_{11} for two-dimensional photonic crystal antenna. Note that the depth of resonance is reduced implying a non-optimal excitation location.

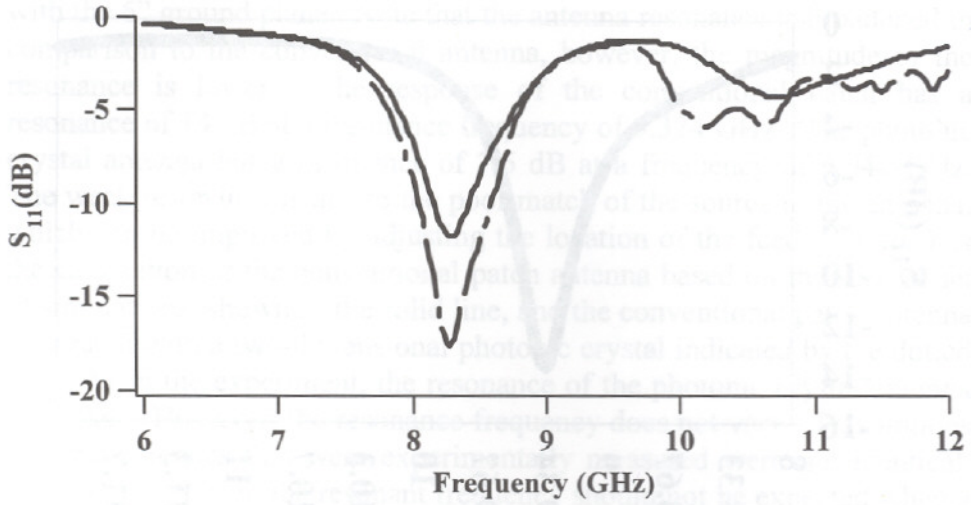

Figure 7. Calculated S_{11} for the conventional patch antenna (dashed line) compared to the two-dimensional photonic crystal antenna (solid line). Note that the resonance is decreased due to a non-optimal excitation location.

5. CONCLUSIONS

A two-dimensional photonic crystal was integrated with a conventional rectangular microstrip patch antenna. The properties of this structure and the effects of a finite sized ground plane on the resonance frequency were studied using an FDTD code. Calculations compare favorably with experiments. For a finite size ground plane, the resonance bandwidth is slightly larger and the resonance is deeper than the case of the infinite size ground plane. Antenna pattern measurements were used to assess the importance of the size of the ground plane. There is an increase in the back lobe level as the ground plane size is reduced. The back lobes are due to energy that propagates away from the antenna in the form of a surface wave and/or a substrate mode. Once the energy reaches the edge of the ground plane, edge currents re-radiate into the back of the antenna. Integration with the photonic crystal reduces the level of the edge currents.

The photonic crystal substrate was fabricated with a defect state under the antenna site. This defect state stores the energy under the antenna. The effects of this defect are currently under investigation. Preliminary results indicate that the radiated power is increased due to the energy

storage under the antenna. Finally, conventional design tools for microstrip patch antennas are insufficient to determine the optimal coupling into the antenna. This is shown in the measurements and calculations that compared the conventional patch antenna to the photonic crystal antenna. A design tool is currently being developed to optimize the incorporation of the antenna with the photonic crystal.

ACKNOWLEGEMENTS

This material is based on work supported by, or in part, by the US Army Research Office under grant number DAAH04-96-1-0439.

REFERENCES

Agi, K., L.D. Moreland, E. Schamiloglu, M. Mojahedi and K.J. Malloy and E.R. Brown, "Photonic Crystals: A New Quasi-optical Component for High-Power Microwaves," *IEEE Trans. on Plasma Science, Sixth Special Issue on High Power Microwave Generation*, vol. 24, no.3, June 1996.

Brown, E.R., C.D. Parker, and O.B. McMahon, "Effect of Surface Composistion on the Radiation Properties from a Photonic-Crystal Planar-Dipole Antenna," *Appl. Phys. Lett.*, vol. 64, June 1994.

Brown, E.R. and O.B. McMahon, "Large Electromagnetic Stop Bands in Metallo-dielectric photonic crystals," *Appl. Phys. Lett.*, Vol. 67, no. 15, Oct. 1995

H. Everitt, Special Issue on "Development and Applications of Materials Exhibiting Photonic Bandgaps," *J. Opt. Soc. Of Amer. B.*, vol. 10, no.2., Feb. 1993.

Joannopoulos, J.D., R.D. Meade and J. N. Winn, *Photonic Crystals: Molding the Flow of Light*, Princeton University Press, New Jersey, 1995.

Kessler, M. P., J.G. Maloney, B.L. Shirley and G. S. Smith, "Antenna Design with the Use of Photonic Band Gap Materials as All Dielectric Planar Reflectors," *Microwave and Opt. Tech. Lett.*, vol. 11, March 1996.

Kunz, K. S., and R.J. Leubbers, *The Finite Difference Time Domain Method for Electromagnetics*, CRC Press, Boca Raton, Florida, 1993.

Pozar, D. M., D. H. Schaubert, *Microstrip Antenna: The Analysis and Design of Microstrip Antennas and Arrays*, IEEE Press, New York, 1995.

Radisic, V., Y. Qian, R. Coccioli and T. Itoh, "Novel 2-D Photonic Bandgap Structure for Microstrip Lines," *IEEE Microwave and Guided Wave Lett.*, Vol. 8, No. 2, pgs 69-71, Feb. 1998.

Remcom, XFDTD is a Registered Trademark of Remcom, Inc., (www.remcom.com).

"The FDTD Method as Implemented in XFDTD," Remcom Inc. short course notes on XFDTD, University Park, PA, March 1998.

Sigalas, M.M., R. Biswas, Q. Li, D. Crouch, W. Leung, R. Jacobs-Woodbury, B. Lough, S. Nielsen, S. McCalmont, G. Tuttle and K.-M. Ho, "Dipole Antennas on Photonic Bandgap Crystals – Experiment and Simulations," *Microwave and Opt. Tech. Lett.*, vol. 15, June 1997.

Taflove, A., *Computational Electromagnetics: The Finite-Difference Time-Domain Method*, Artech House, Norwood, MA, 1995.

Yang, H.Y. D., N. G. Alexopoulos and E. Yablonovitch, "Photonic Band-Gap Materials for High-Gain Printed Circuit Antennas," *IEEE Trans. on Ant. and Prop.*, vol. 45, no. 1, January 1997.